

CONF-8411142-1

MANY-ELECTRON EFFECTS IN ELECTRON-IMPACT IONIZATION
OF MULTIPLY CHARGED IONS

R. A. Phaneuf

CONF-8411142--1

Oak Ridge National Laboratory*
Oak Ridge, TN 37831

DE85 005570

Proceedings of Second International Workshop
on Cross Sections for Fusion and Other Applications
College Station, Texas
November 8-10, 1984

To be published in
Nuclear Instruments and Methods in Physics Research
April 1985

DISCLAIMER

This report was prepared as an account of work sponsored by an agency of the United States Government. Neither the United States Government nor any agency thereof, nor any of their employees, makes any warranty, express or implied, or assumes any legal liability or responsibility for the accuracy, completeness, or usefulness of any information, apparatus, product, or process disclosed, or represents that its use would not infringe privately owned rights. Reference herein to any specific commercial product, process, or service by trade name, trademark, manufacturer, or otherwise does not necessarily constitute or imply its endorsement, recommendation, or favoring by the United States Government or any agency thereof. The views and opinions of authors expressed herein do not necessarily state or reflect those of the United States Government or any agency thereof.

*This research was supported by the Office of Fusion Energy of the U.S. Department of Energy under contract No. DE-AC05-84OR21400 with Martin Marietta Energy Systems, Inc.

MASTER

DISTRIBUTION OF THIS DOCUMENT IS UNLIMITED

EDB

MANY-ELECTRON EFFECTS IN ELECTRON-IMPACT IONIZATION
OF MULTIPLY CHARGED IONS

R. A. Phaneuf

Oak Ridge National Laboratory
Oak Ridge, TN 37831

ABSTRACT

Many-electron phenomena critically influence the ionization of multiply charged ions by electron impact. In general, inner-shell electrons play an increasingly important role in the electron-impact ionization process as the ionic or nuclear charge increase along an ionic sequence. A few specific examples are given to illustrate the signature and relative contributions of a number of indirect ionization mechanisms to the total ionization cross sections.

1. INTRODUCTION

The stimulus of the fusion program and the availability of improved ion sources continue to produce a significant expansion of the base of accurate experimental data for electron-impact ionization of multiply charged ions. Systematization of experimental and theoretical studies along isoelectronic (same electronic structure), isonuclear (same species) or isoionic (same charge) sequences have identified new ionization mechanisms and produced an enhanced level of understanding of the ionization process. In many cases, the cross section for these so-called indirect ionization channels dominate by more than an order of magnitude that for direct ejection of an outer-shell electron. These indirect mechanisms may be generally classified as many-electron effects, since in each case, more

than one initially-bound ionic electron plays a role in the ionization process via the autoionization or Auger process. There is also some experimental suggestion of correlated behavior of ionic electrons in multiple ionization in a single collision.

In this paper, a few examples will be given which illustrate the role of several different ionization mechanisms, and an attempt will be made to characterize some of the trends which are emerging from systematic studies along ionic sequences.

2. IONIZATION MECHANISMS

a. Direct Ionization

Direct ionization refers to a transition from a bound state directly to the continuum, with no other excited bound or quasi-bound levels playing a role. The projectile electron directly ejects an electron from the ion, most commonly from the outer or valence shell:



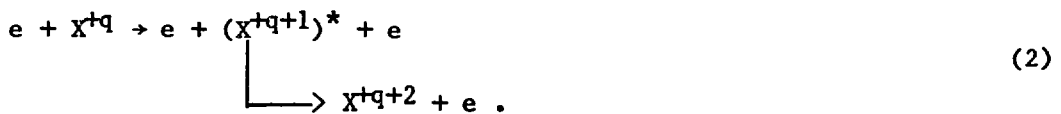
This usually produces a single ionization event ($n=1$), since the probability of a projectile electron causing the direct ejection of more than one ionic electron is relatively small. The direct ejection of an inner-shell electron leaves the ionized ion in an excited state. The process is usually classified as direct ionization if the "hole" state decays radiatively rather than by subsequent Auger emission.

Direct ionization cross sections may be estimated quite reliably by first-order quantum-mechanical perturbation treatments such as the distorted-wave Born approximation [1,2]. The Lotz semiempirical formula [3] is also widely used, and has been shown to predict direct ionization

cross sections to much better than a factor of two in most cases. A typical example relevant to fusion research is shown in Figure 1, where experimental cross sections [4] for electron-impact ionization of Fe^{2+} are compared to distorted-wave calculations [5] and to the Lotz prediction. The agreement in magnitude, and particularly in shape with the distorted-wave calculation is favorable, except at the lowest energies, where the onset of the experimental ionization cross section reflects the population in the reacting beam of low-lying metastable levels within the $3d^6$ ground-state configuration.

b. Ionization-Autoionization

As noted above, the ejection of a more tightly bound inner-shell electron leaves an excited ion which can subsequently autoionize, resulting in the ejection of one or more additional electrons, depending on the excitation energy of the "hole" state, and the branching ratio for radiative versus Auger decay (fluorescence yield). This indirect process is usually referred to as ionization-autoionization, and is the dominant mechanism for net multiple ionization in most cases:



In this example, the excited state $(X^{+q+1})^*$ decays by single autoionization yielding net double ionization. For deeper inner-shell vacancies, successive Auger emissions, or simultaneous multiple Auger emissions may also be possible, resulting in net multiple ionization.

Figure 2, taken from a recent paper of Pindzola et al. [6], compares experimental cross sections [6,7] for electron-impact double ionization in

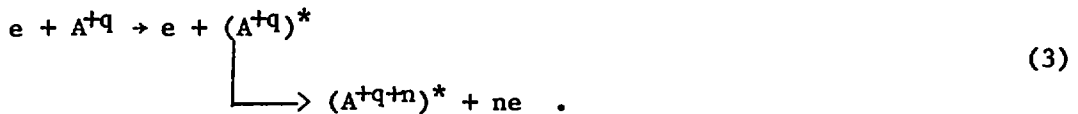
the isonuclear sequence Ar^{2+} , Ar^{3+} , and Ar^{4+} . The comparison demonstrates the increasing dominance of the 2p ionization-autoionization mechanism in the net double-ionization cross section relative to direct-double ionization as the ionic charge increases. This trend is expected to continue along the isonuclear sequence through Ar^{6+} , with the double ionization cross section remaining roughly constant in magnitude, and equal to that for 2p ionization. The double-ionization threshold of Ar^{7+} increases to 566 eV, and ejection of a 2p electron can no longer produce double ionization via the ionization-autoionization mechanism.

A number of possible ionization-autoionization channels in the multiple ionization of Xe^{6+} are shown in Figure 3, where calculated Hartree-Fock energy thresholds [8] for the production of various inner-shell and multiple outer-shell vacancies are indicated relative to the $3d^{10}4s^24p^64d^{10}5s^2$ ground state of Xe^{6+} . For example, ejection of a 4d electron from Xe^{6+} can lead only to single ionization, whereas 4p ionization can lead to double ionization via the ionization-autoionization mechanism. Figure 4 compares experimental cross sections [9] for single, double, and triple ionization of Xe^{6+} with Lotz predictions for the sum of cross sections for 5s and 4d ionization for σ_{67} , for 4s and 4p ionization for σ_{68} , and 3d ionization for σ_{69} . The single ionization cross section, σ_{67} , is dominated by excitation-autoionization channels, and will be discussed in the following section. The experimental double-ionization cross section onset is consistent with 195 eV, which is the minimum energy required to remove two 5s electrons, and significantly below the 4p ionization-autoionization threshold of 242 eV. Similarly, the triple ionization cross section, σ_{69} , shows an onset which is significantly below

the 3d ionization threshold of 764 eV, which is the lowest ionization-autoionization channel which can produce net triple ionization. Thus, for both σ_{68} and σ_{69} , there is experimental evidence for the direct ejection of two or three outer-shell electrons. Cross sections for such a "direct multiple knockout" mechanism may be estimated using the semiclassical binary-encounter approximation [10], and are predicted to be negligible compared to the observed cross sections in both cases. The mechanisms which are responsible for these observations are not understood, but are suggestive of correlated or collective behavior of the ionic electrons.

c. Excitation-Autoionization

Contributions to the ionization of a multiply charged ion produced by the excitation of an ionic inner-shell electron to an autoionizing state were first identified for Li-like ions by Crandall et al. [11]. This mechanism may be represented as follows:



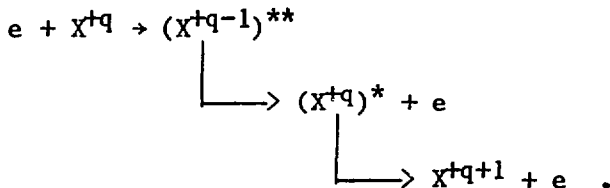
A number of examples of this mechanism have been documented, and it has been shown to dominate the single ionization cross sections for Ti^{3+} , Zr^{3+} , and Hf^{3+} by more than an order of magnitude [12]. Reasonable agreement has been obtained with experiment in many cases by simply adding theoretical cross sections for the appropriate excitation process to the direct ionization cross section, ignoring possible interference effects between these channels. Because the cross section for excitation of an ion by electron impact is finite and most often largest at its threshold energy, the excitation-autoionization process for a strong, well-isolated transition

produces a distinctive and readily identifiable signature in the ionization cross section. In Figure 5, taken from a recent paper by Griffin et al. [13], experimental cross sections for five members of the Xe-isonuclear sequence are compared to distorted-wave theoretical calculations for direct ionization. Although the peak experimental cross sections decrease slowly with increasing ionic charge, they become increasingly larger than the direct-ionization theory as the ionic charge increases from 2 to 6. This enhancement is attributed to inner-shell excitations to autoionizing levels of the types $Xe^{+q} (4d^1 0s^2 5p^{6-q}) \rightarrow Xe^{+q} (4d^9 5s^2 5p^{6-q} n\ell)$ with $n\ell = 4f, 5p, 5d$, and $5f$. Hartree-Fock atomic structure calculations for the $4d^9 5s^2 5p^{6-q} nf$ configurations are highly term-dependent, and this was found to have a pronounced effect on the magnitude and energy dependences of the distorted-wave calculations of cross sections for these excitation-autoionization contributions. Very reasonable agreement was realized between detailed theoretical calculations and experiment for these isonuclear ions, both with regard to the excitation energies and the magnitudes of the cross sections for the various excitations. The pronounced "hump-like" features in Xe^{2+} and Xe^{3+} occur because of the dominance of non-dipole-allowed excitations for these cases. The cross sections for such transitions are expected to fall off asymptotically as $1/E$ for dipole-forbidden excitations, and as $1/E^3$ for spin-forbidden excitations, whereas cross sections for both dipole-allowed excitations and for direct ionization fall off much more slowly, as $\ln E/E$ [14]. Thus the signature of an excitation feature in the ionization cross section gives useful information about both the threshold energy and the nature of the excitation process which leads to autoionization. Coupled with a branching ratio for

autoionization versus radiative decay, this signature can provide a quantitative basis for evaluating theoretical methods for electron-impact excitation cross section calculations. This can be particularly valuable, since direct excitation cross section measurements for ions, and particularly multiply charged ions, are technically very difficult, and few in number.

d. Resonant-Recombination Double Autoionization

In 1981, LaGattuta and Hahn [15] postulated an ionization mechanism whereby the projectile electron resonantly recombines with the target ion to form a doubly-excited intermediate state, which subsequently decays by two-step Auger emission:



This seemingly exotic ionization mechanism was predicted to make a non-negligible contribution to the total ionization cross section for Fe^{15+} . Henry and Msezane [16] have suggested a variation whereby the doubly-excited intermediate state decays by simultaneous double Auger emission, which they have labeled "auto-double ionization."

The resonant process here is analogous to dielectronic recombination, except that it is associated with the excitation of an inner-shell electron. Assume that an electron approaches an ion with just less than the energy required to excite a transition in the ion. Kinetic-energy gain due to acceleration by the Coulomb field of the ion may allow the electron to excite the ion, but the electron is now trapped by the Coulomb field, and is captured into a doubly-excited Rydberg level. The doubly excited ion

can either radiate away some of the excess energy, stabilizing the recombination, or can autoionize. If the excitation involves an inner-shell electron, sequential or simultaneous double autoionization may be energetically possible. The signature for this process is expected to be the same as that for dielectronic recombination, i.e., the cross section consists of a Rydberg series of sharp resonances just below and converging to the threshold energy of the relevant excitation. The expected effect on an experimental electron-impact ionization cross section measurement with finite electron energy resolution is a smearing-out of the sharp onset of an excitation feature to energies below the expected excitation threshold. In Figure 6, taken from ref. [13], theoretical distorted-wave calculations for both direct ionization and excitation-autoionization are summed and compared to the experimental data. Experiment and theory are in nearly perfect agreement at energies above the cross-section maximum at 85 eV, but the experimental ionization cross section shows significant enhancement over direct ionization at energies below the range of predicted excitation thresholds. Although no specific calculations have yet been performed, similar features are present in other members of the Xe isonuclear sequence, and are suggestive of the resonant mechanism.

3. SUMMARY

Many-electron phenomena play an important role in the electron-impact ionization of multiply charged ions. Through systematic experimental and theoretical investigations along ionic sequences, a number of indirect ionization mechanisms have been identified and accurately quantified in many cases. In general, as the ionic charge increases along an isonuclear

sequence, these indirect ionization channels and the role of inner electronic shells become progressively more important. Similarly, multiple ionization is dominated by inner-shell ionization-autoionization and becomes relatively more important with increasing ionic charge. There is some indication that correlated or collective electron behavior may in some cases play a role in multiple ionization by electron impact. Experimental evidence also suggests that more exotic indirect ionization mechanisms such as resonant-recombination multiple autoionization may also make a significant contribution to the total ionization cross section in some cases. The increasing level of systematic experimental and theoretical activity on this subject promises to resolve some of these puzzles, and uncover new ones in the process.

ACKNOWLEDGMENTS

The author is indebted to D. C. Gregory, A. M. Howald, and D. H. Crandall, who are or have been recent members of the ORNL electron-ion experimental team. A number of these measurements were performed in continuing collaboration with G. H. Dunn and members of his JILA research group (D. W. Mueller and T. J. Morgan).

The ORNL theoretical atomic physics for fusion group of C. Bottcher, D. C. Griffin, and M. S. Pindzola continue to provide the theoretical background and much of the inspiration for this work. This research was supported by the Office of Fusion Energy of the U.S. Department of Energy under contract No. DE-AC05-84OR21400 with Martin Marietta Energy Systems, Inc.

REFERENCES

1. S. M. Younger, Phys. Rev. A 22, 111 (1980).
2. M. S. Pindzola, D. C. Griffin, and C. Bottcher, J. Phys. B 16, 2355 (1983).
3. W. Lotz, Z. Physik 206, 205 (1967); *ibid* 220, 466 (1969).
4. D. W. Mueller, T. J. Morgan, G. H. Dunn, D. C. Gregory, and D. H. Crandall, "Absolute cross section measurements for electron-impact ionization of twice-charged ions: Ti^{2+} , Fe^{2+} , Ar^{2+} , Cl^{2+} , and F^{2+} ," Phys. Rev. A (submitted 1984).
5. M. S. Pindzola, D. C. Griffin, C. Bottcher, D. C. Gregory, A. M. Howald, R. A. Phaneuf, D. H. Crandall, G. H. Dunn, D. W. Mueller, and T. J. Morgan, Oak Ridge National Laboratory Report ORNL/TM-9436 (January 1985).
6. M. S. Pindzola, D. C. Griffin, C. Bottcher, D. H. Crandall, R. A. Phaneuf, and D. C. Gregory, Phys. Rev. A 29, 1749 (1984).
7. A. Müller and R. Frodl, Phys. Rev. Lett. 44, 29 (1980).
8. M. S. Pindzola, private communication (1983).
9. A. M. Howald, D. C. Gregory, D. H. Crandall, and R. A. Phaneuf, unpublished data, ORNL (1984).
10. M. Gryzinski, Phys. Rev. 138, A336 (1965).
11. D. H. Crandall, R. A. Phaneuf, B. E. Hasselquist, and D. C. Gregory, J. Phys. B 12, L249 (1979).
12. R. A. Falk, G. H. Dunn, D. C. Gregory, and D. H. Crandall, Phys. Rev. A 27, 762 (1983).
13. D. C. Griffin, C. Bottcher, M. S. Pindzola, S. M. Younger, D. C. Gregory, and D. H. Crandall, Phys. Rev. A 29, 1729 (1984).

14. W. D. Robb, "Theoretical Studies of Electron Impact Ionization," pp. 245-265 in Atomic and Molecular Processes in Controlled Thermonuclear Fusion, eds., M.R.C. McDowell and A. M. Ferendeci, Plenum, New York, 1980.
15. K. J. LaGattuta and Y. Hahn, Phys. Rev. A 24, 2273 (1981).
16. R.J.W. Henry and A. Z. Msezane, Phys. Rev. A 26, 2545 (1982).

FIGURE CAPTIONS

Figure 1. Experimental and theoretical cross sections versus electron energy for electron-impact ionization of Fe^{2+} . The dashed curve represents the Lotz semiempirical formula [3] and the solid curve the Coulomb-distorted-wave calculation of Pindzola et al. [5] for direct ionization. The experimental data are those of Mueller et al. [4].

Figure 2. Comparison of electron-impact double-ionization cross sections in the Ar isonuclear sequence, from ref. 6. The open circles and triangles are experimental data of Müller et al. [7] for Ar^{2+} and Ar^{3+} , respectively; and solid circles are measurements of Crandall et al. [6] for Ar^{4+} . Solid curve is a distorted-wave calculation of Pindzola et al. [6] for ionization of a 2p electron in Ar^{4+} .

Figure 3. Hartree-Fock theoretical energy thresholds from Pindzola [8] for ionization of various subshells in the Xe isonuclear sequence. The energy scale is relative to the $3d^{10}4s^24p^64d^{10}5s^2$ ground state of Xe^{6+} . The tops of the cross-hatched bars designate the ionization potentials of each stage, and downward arrows designate possible autoionization pathways.

Figure 4. Experimental cross sections versus electron energy [9] for electron-impact single (σ_{67}), double (σ_{68}), and triple (σ_{69}) ionization of Xe^{6+} . The vertical arrows designate the minimum threshold energies for each process. The dashed curves are the sum of Lotz semiempirical cross sections for 5s and 4d ionization which contribute to σ_{67} , for 4s and 4p ionization which contribute to σ_{68} , and for 3d ionization in the case of σ_{69} .

Figure 5. Comparison of experimental cross sections and distorted-wave direct-ionization calculations for electron-impact single ionization in the Xe-isonuclear sequence, from Griffin et al (ref. 13).

Figure 6. Comparison of experimental and theoretical cross sections for electron-impact ionization of Xe^{3+} near threshold. Long-dashed curve is the distorted-wave direct ionization calculation. Solid curve represents distorted-wave cross sections for excitation autoionization added to the direct cross section. The short-dashed curve is a convolution of the solid curve with a 2 eV FWHM Gaussian to model the finite experimental energy spread. Arrows designate ranges of threshold energies for the excitations to autoionizing levels in the configurations indicated.

Fig. 1

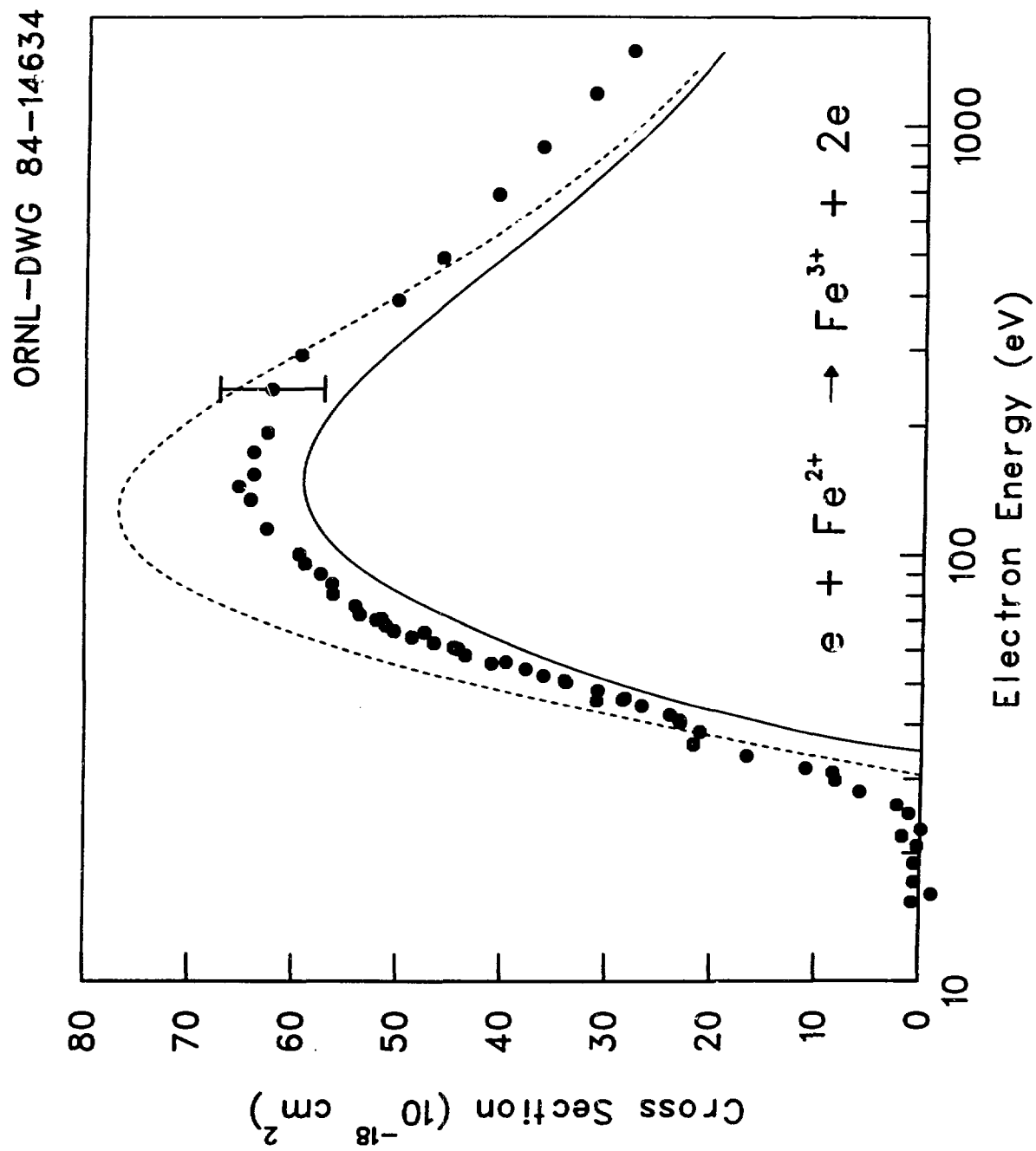


Fig. 2

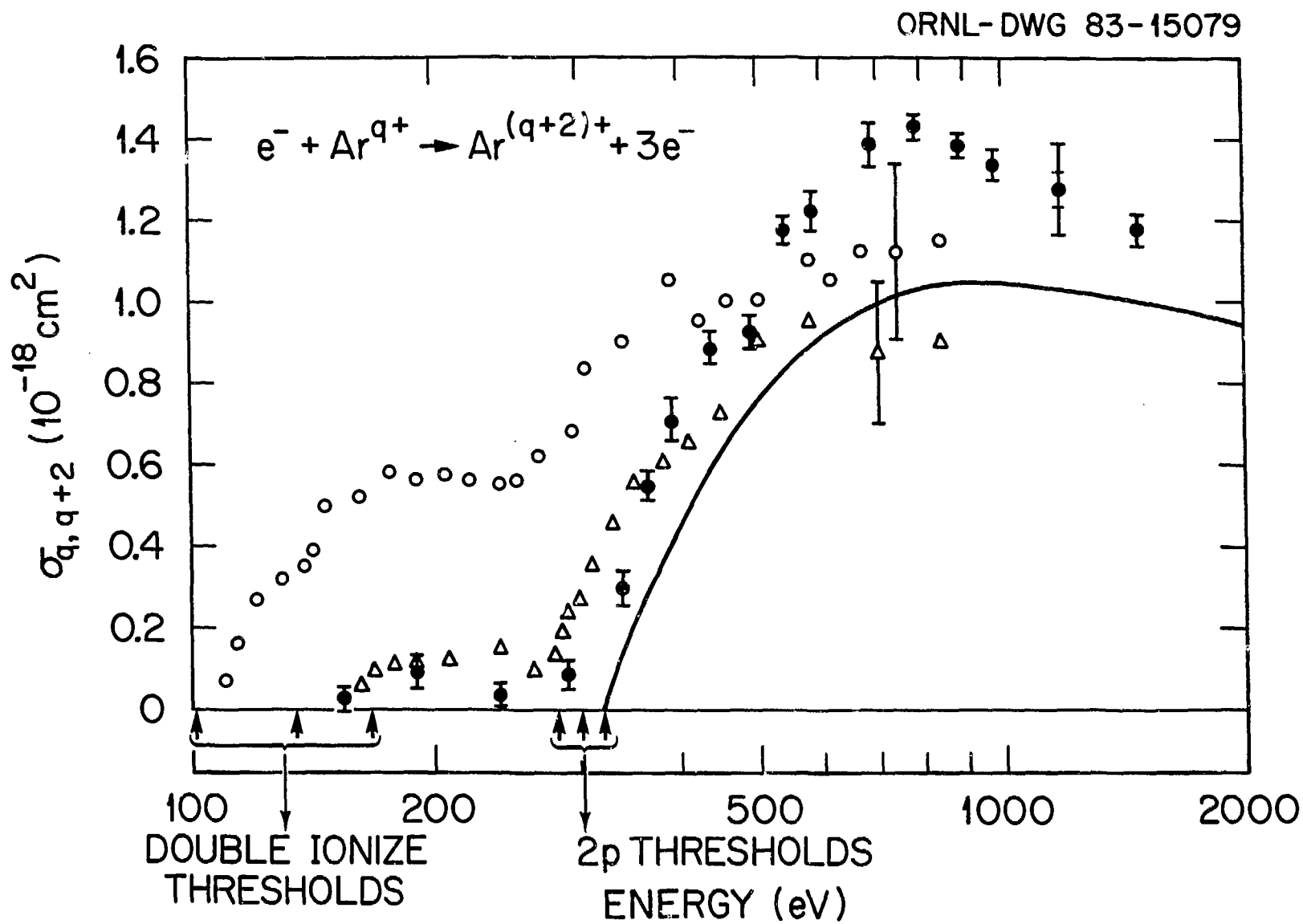


Fig. 3

ORNL-DWG 84-10641

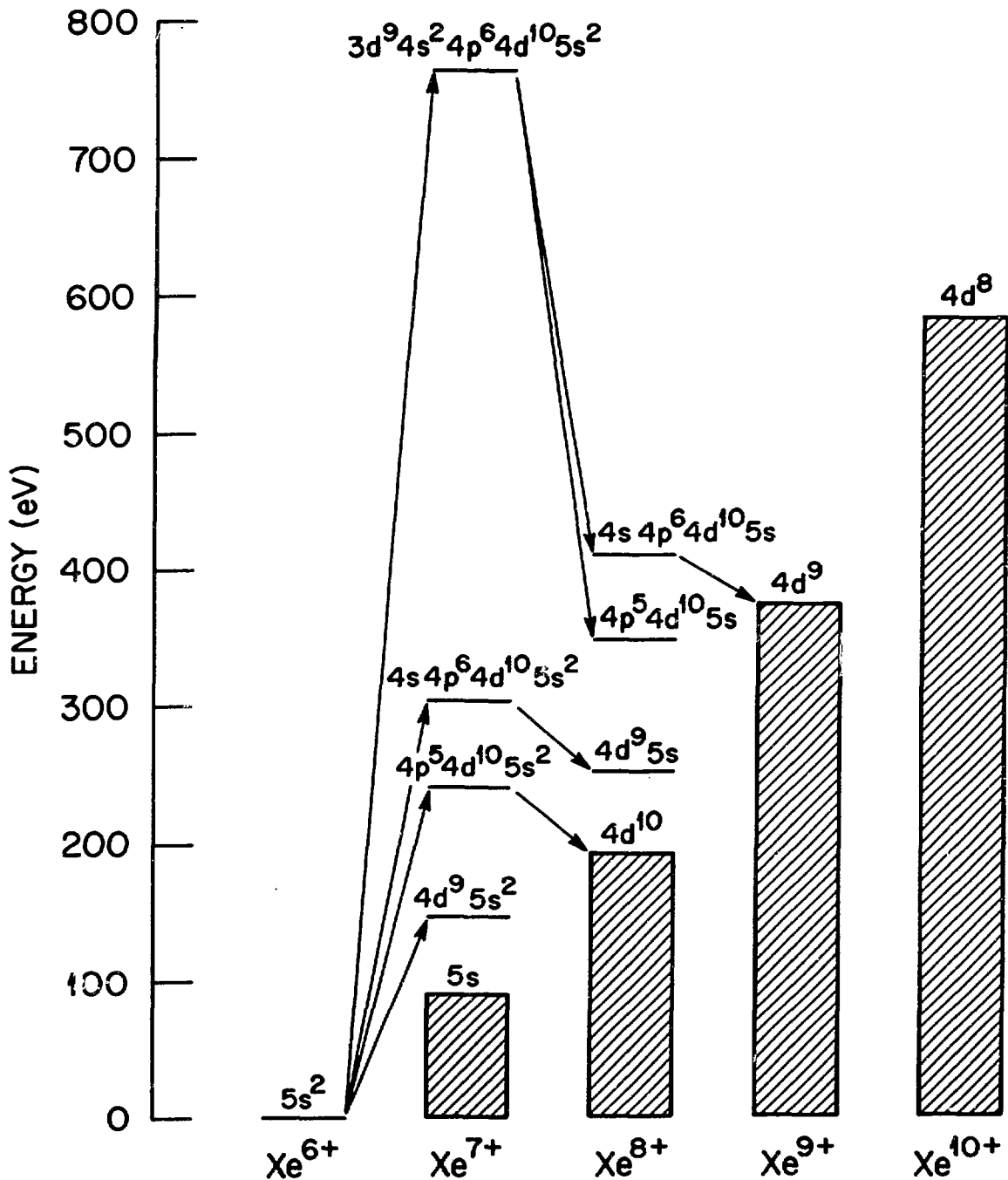


Fig. 4

ORNL-DWG 84-10644R

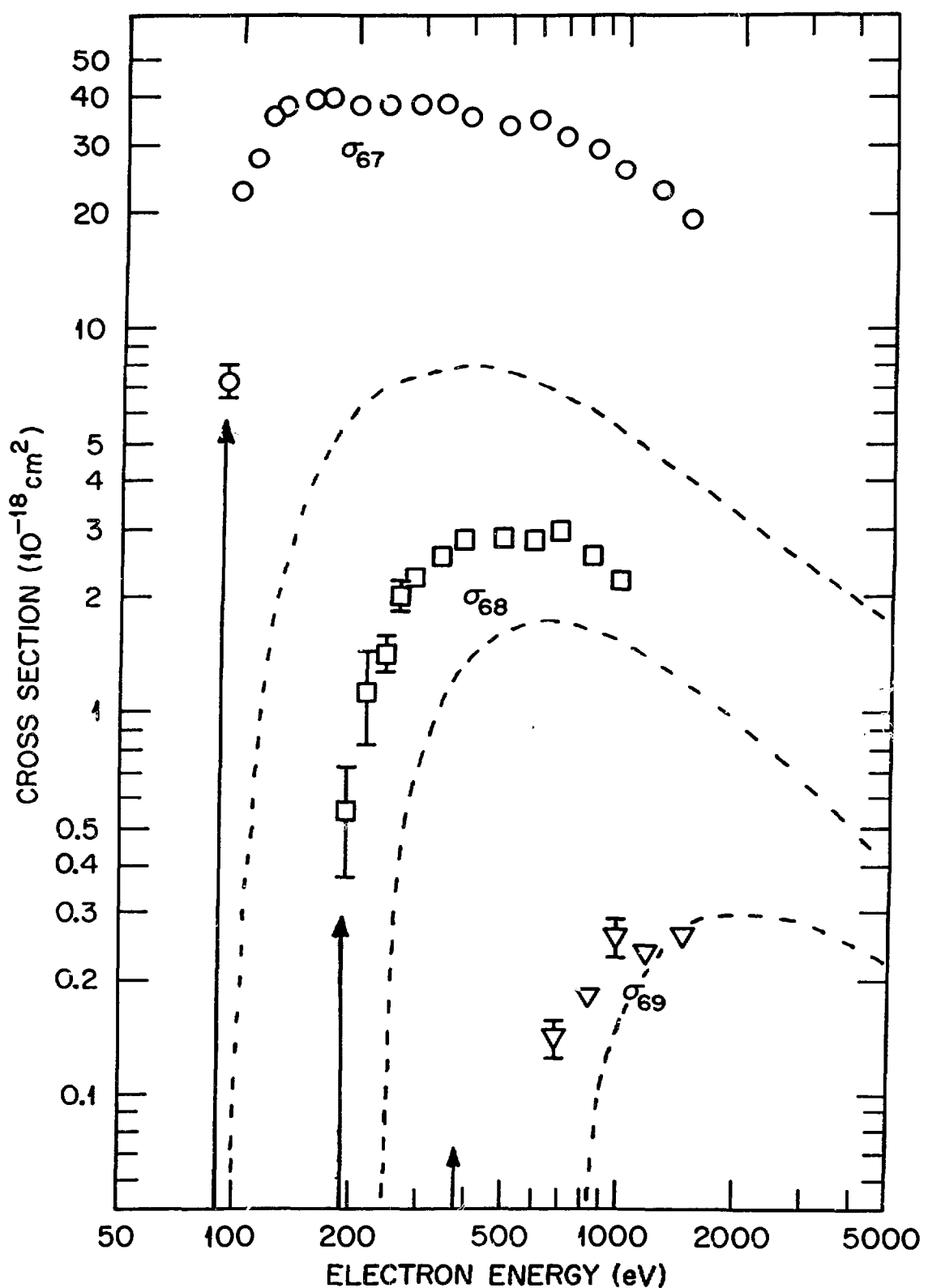


Fig. 5

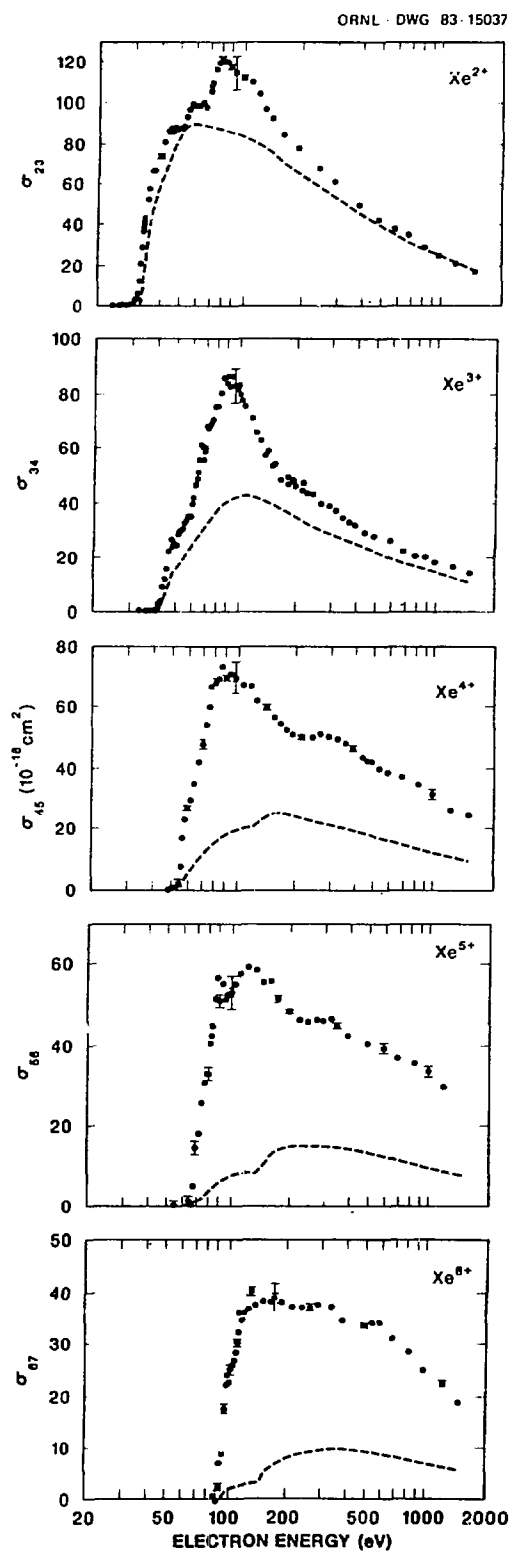


Fig. 6

